Dual-head gamma camera 2-[fluorine-18]-fluoro-2-deoxy-D-glucose positron emission tomography in oncological patients: effects of non-uniform attenuation correction on lesion detection

M. Zimny, H.J. Kaiser, U. Cremerius, P. Reinartz, M. Schreckenberger, O. Sabri, U Buell

Department of Nuclear Medicine, University Hospital, Aachen University of Technology, Pauwelsstrasse 30, D-52074 Aachen, Germany

Received 9 April and in revised form 20 April 1999

Abstract. The purpose of this study was to evaluate a dual head coincidence gamma camera (DH-PET) equipped with single-photon transmission for 2-[fluorine-18]-fluoro-2-deoxy-D-glucose (FDG) imaging in oncological patients. Forty-five patients with known or suspected malignancies, scheduled for a positron emission tomography (PET) scan, were first studied with a dedicated ring PET and subsequently with DH-PET. All patients underwent measured attenuation correction using germanium-68 rod sources for ring PET and caesium-137 sources for DH-PET. Ring PET emission scan was started 64±17 min after intravenous administration of 235±42 MBq FDG. DH-PET emission followed 160±32 min after i.v. FDG. Attenuation-corrected and non-attenuation-corrected images were reconstructed for ring PET and DH-PET. The image sets were evaluated independently by three observers blinded to clinical data and to results of conventional imaging. Attenuation-corrected ring PET as the standard of reference depicted 118 lesions, non-attenuation-corrected ring PET 113 (96%) lesions, and attenuation-corrected DH-PET and non-attenuation-corrected DH-PET, 101 (86%) and 84 (71%) lesions, respectively ($P<0.05$). The lesion detection rate of attenuation-corrected and non-attenuation-corrected DH-PET was almost similar for lesions >20 mm, whereas attenuation correction increased the detection rate from 60% to 80% for lesions ≤20 mm ($P<0.01$). A patient-based analysis revealed concordant results relative to attenuation-corrected ring PET for non-attenuation-corrected ring PET, attenuation-corrected DH-PET and non-attenuation-corrected DH-PET in 42 (93%), 36 (80%) and 31 (69%) patients, respectively. Differences might have influenced patient management in two (4%), six (13%) and ten (22%) patients, respectively. In conclusion, measured attenuation correction markedly improves the lesion detection capability of DH-PET. With measured attenuation correction the diagnostic performance of DH-PET is closer to that of dedicated ring PET.

Key words: Dual-head gamma camera – Positron emission tomography – Attenuation correction – Oncological patients

Eur J Nucl Med (1999) 26:818–823

Introduction

Today positron emission tomography (PET) with 2-[fluorine-18]-fluoro-2-deoxy-D-glucose (FDG) plays an important role in the diagnostic work-up of oncological patients [1]. However, this method is cost-intensive, hindering its widespread use [2]. This has led to the development of gamma cameras suitable for both conventional single-photon imaging and positron imaging. Previous studies have shown that FDG imaging in oncological patients is possible with gamma cameras equipped with ultra-high-energy collimators [3–10]. However, Macfarlane et al. reported a lower system sensitivity and spatial resolution for single-photon emission tomography (SPET) systems compared with ring PET and a limited detectability of hypermetabolic lesions with a diameter below 2–3 cm [5]. Lonneux et al. compared FDG SPET and ring PET in lung cancer and gastrointestinal malignancies and concluded that FDG SPET cannot substitute for ring PET in oncological patients [11].

Recently dual-head gamma cameras modified for coincidence detection have become available for oncological FDG PET imaging. These systems provide both higher spatial resolution and system sensitivity compared with SPET systems [12]. Phantom studies revealed a spatial resolution comparable to that of ring PET, while

Correspondence to: M. Zimny, Department of Nuclear Medicine, University Hospital, Aachen University of Technology, Pauwelsstrasse 30, D-52074 Aachen, Germany

system sensitivity and lesion detection capability for dual-head coincidence gamma cameras are still inferior to dedicated ring PET [13–15]. Despite these limitations, Stokkel et al. reported encouraging clinical results for dual-head gamma camera PET in 11 patients with laryngeal cancer [16]. In contrast, Shreve et al. demonstrated a limited value of gamma camera PET for FDG imaging compared with ring PET, the lesion detection rate for gamma camera PET being only 55% [12]. Delbeke et al. showed a relative sensitivity for a dual-head gamma camera system of 73% in 19 patients [14]. This is confirmed by our previously published results showing a lesion detection rate of 79% in 32 oncological patients. In agreement with Delbeke et al., we assumed that the lack of non-uniform attenuation correction is a possible reason for this apparent limitation of DH-PET [15].

Transmission scanning using the single-photon source caesium-137 was introduced for PET by Karp et al. and Yu et al. in 1995 [17, 18]. Potential advantages of singles transmission compared with coincidence transmission using germanium-68 sources are the shorter acquisition time and the possibility of discriminating transmission and emission events due to the energy of ^{137}Cs of 662 keV [17]. Recently, measured attenuation correction was introduced for DH-PET using singles transmission with collimated ^{137}Cs point sources [19].

The aim of the present study was to evaluate whether measured attenuation correction using singles transmission is helpful in overcoming lesion detection limitations of dual-head gamma camera PET using dedicated ring PET as the standard of reference.

Materials and methods

This study comprised 45 oncological patients with a mean age of 57±14 years who were scheduled for a PET scan. Suspected or known diagnosis was malignant lymphoma (*n*=10), head and neck cancer (*n*=10), lung cancer (*n*=7), recurrent colorectal cancer (*n*=4), pancreatic cancer (*n*=4), ovarian cancer (*n*=2), cervical cancer (*n*=3), malignant melanoma (*n*=1), germ cell cancer (*n*=1), renal cell cancer (*n*=2) and cancer of unknown primary (*n*=1). Prior to PET, all patients were in a fasted state for at least 6 h, controlled by serum glucose levels.

Ring PET. The emission ring PET scan (ECAT EXACT, CTI Knoxville, Tenn.) was started 64±17 min after intravenous administration of 235±42 MBq FDG. The ring PET studies were performed as whole-body scans in all patients except those with head and neck cancer. For the whole-body scan the scan field comprised five or six bed positions, while in patients with head and neck cancer the scan field comprised two bed positions. All patients underwent measured attenuation correction using ^{68}Ge rod sources. For repositioning of the patients a laser guide system was used. The acquisition time was 10–15 min per bed position for the emission scan and 12–15 min for the transmission scan. All studies were performed with extended septa (2D mode). Attenuation-corrected images were reconstructed using iterative reconstruction based on the maximum likelihood expectation maximisation algorithm [20]. Filtered backprojection was used to reconstruct non-attenuation-corrected images since the iterative algorithm established in our laboratory reduces the image quality of non-attenuation-corrected images (data not shown).

Dual-head gamma camera PET (DH-PET). DH-PET was performed on the same day following the ring PET study using a dual-head gamma camera modified for coincidence detection (Solus MCD/AC, ADAC Labs., Milpitas, Calif.). To improve efficiency for the detection of 511-keV photons, the detectors are equipped with 5/8-inch sodium iodine crystal instead of the regular 3/8-inch crystal. In coincidence mode stray radiation shields are mounted on each detector to decrease radiation from outside the field of view. For single-photon transmission scanning both detectors are equipped with collimated ^{137}Cs point sources with an activity of 30 mCi each.

The gamma camera was positioned according to the known or suspected disease. The DH-PET study consisted of one bed position in all patients (38.5 cm axial). For the emission scan data were acquired with a 180° rotation with 32 steps of pre-set 40 s each. Decay correction was performed by automatically adjusting the time of each acquisition step. A dual-window technique was used, accepting coincidences between photopeak events and photopeak and Compton events. This technique increases the coincidence rate but also results in an increase in scattered and random events [21]. The pre-set windows (photopeak 511 keV±15%, Compton 310 keV±15%) were adjusted for each patient study. The Compton window was set relative to the photopeak window according to the manufacturer's guidelines. The acquisition matrix was 128×128. For reconstruction the data were rebinned into 96 projections.

The emission scan was started 160±32 min after intravenous administration of FDG IV and was immediately followed by a transmission scan with the patient in the identical position. The acquisition consisted of a 360° rotation with 96 azimuths of 2 s each. To cover the axial field of view, both point sources translate axially along the detectors. The pre-set window (662 keV±10%) was adjusted for each patient study. Total acquisition time (emission and transmission) for one bed position was about 30 min. The increase in acquisition time of 6 min/bed position is acceptable and was well tolerated by the patients.

After prefiltering with a Wiener filter, the data were reconstructed iteratively with and without attenuation correction using software provided by the manufacturer (ordered subsets expectation maximisation; eight subsets, two steps). Figure 1 shows a coronal slice of the thorax without attenuation correction and with attenuation correction, and the corresponding attenuation map.

Image analysis. All four image sets (ring PET with/without attenuation correction and DH-PET with/without attenuation correction) were evaluated independently by three observers using an interactive grey-scaled screen display. The observers were blinded to the results of conventional imaging and to clinical data. The number of detectable lesions with focally increased FDG uptake outside the physiological pattern as criterion of malignancy was counted or each image set. Consensus was obtained for each lesion by majority decision. The detection rate of each modality was calculated relative to attenuation-corrected ring PET as the standard of reference. Attenuation-corrected ring PET images were used to assess the lesion size applying the "measure distance tool" implemented in the ECAT 6 software package. Additionally, lesion-to-background ratios were determined for attenuation-corrected and non-attenuation-corrected ring PET and DH-PET imag-

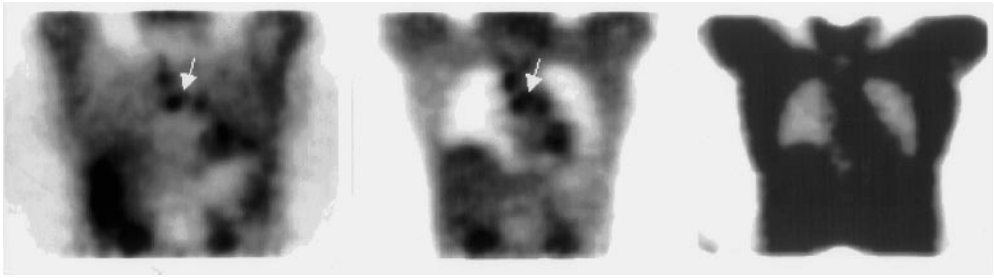

Fig. 1. Corresponding coronal DH-PET images of the thorax and the upper abdomen: without attenuation correction (*left*) and with attenuation correction (*middle*). The *right image* shows the attenuation map. With attenuation correction, anatomical structures like the lungs and the mediastinum are better delineated. Without attenuation correction the FDG uptake in the lungs and the peripheral parts of the liver is overestimated. These artefacts are not visible after attenuation correction. Note also the better demonstration of the small mediastinal lesion located in the midline (*white arrow*)

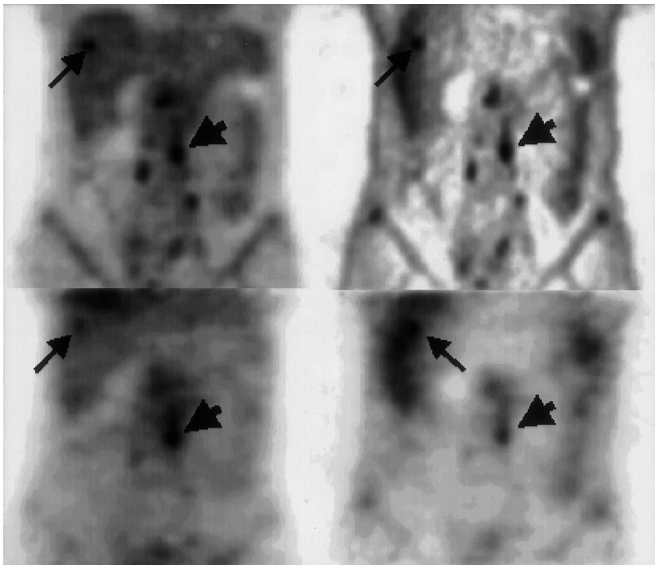

Fig. 2. Corresponding coronal slices of attenuation-corrected ring PET (*top left*), non-attenuation-corrected ring PET (*top right*), attenuation-corrected DH-PET (*bottom left*) and non-attenuation-corrected DH-PET (*bottom right*). *Thick arrow*, para-aortic lymph node involvement; *thin arrow*, focal liver lesion. The liver lesion is clearly shown with ring PET and attenuation-corrected DH-PET; however, it is hardly visible with non-attenuation-corrected DH-PET

es using identical regions of interest. Standardised uptake values (SUVs) normalised to body weight were calculated for each lesion approximately corrected for partial volume effects using attenuation-corrected ring PET image data [22]. A patient-based analysis of the findings of each image set was performed to assess the clinical significance of differences in lesion detection.

Statistical analysis. Data are presented as mean±standard deviation. The Mann-Whitney *U* test was used to compare differences between unpaired samples, Wilcoxon's test to compare differences between paired samples, and the chi square test to compare frequencies (SPSS for Windows, SPSS Inc.).

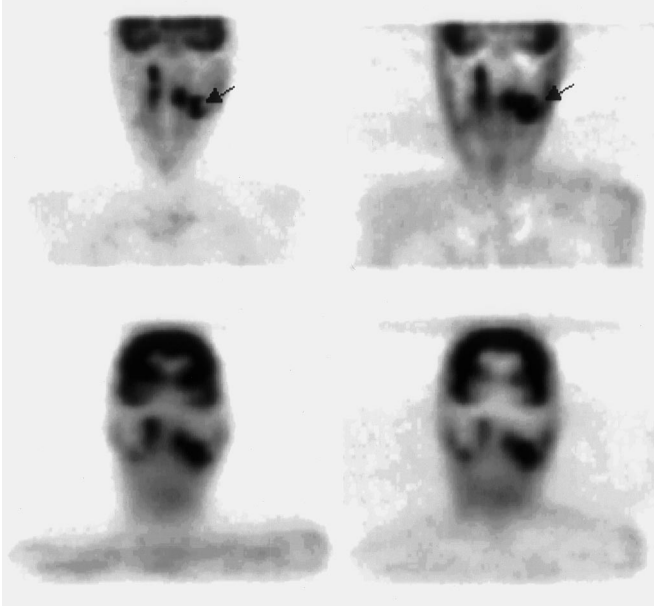

Fig. 3. Head and neck cancer with bilateral lymph node metastases shown with ring PET and DH-PET. However, central necrosis is best demonstrated with attenuation-corrected ring PET (*arrow*). Sequence of images as in Fig. 2

Results

An example of the improved image quality of attenuation-corrected DH-PET is given in Fig. 1. The anatomical structures of the thorax and the upper abdomen are clearly delineated only with attenuation correction. Furthermore, the artefacts of the non-attenuation-corrected image, such as increased activity in the lungs and at the liver surface, are compensated by measured attenuation correction. Figure 2 shows a patient with multiple abdominal lesions. All lesions are clearly shown with attenuation-corrected and non-attenuation-corrected ring PET. However, the liver lesion, clearly demonstrated with attenuation-corrected DH-PET, is hardly visible with non-attenuation-corrected DH-PET. Figure 3 shows a patients with head and neck cancer and bilateral lymph node metastases demonstrated by ring PET and DH-PET.

Attenuation-corrected ring PET detected 118 lesions in 37 out of 45 patients. Eight patients showed no focally increased FDG uptake and were regarded as free of malignancy. Non-attenuation-corrected ring PET demon-

Table 1. Detection rate and anatomical region

Region	Ring PET		DH-PET		*P* value
	AC (*n*)	no AC	AC	no AC	
Head/neck	18	17/18 (94%)	16/18 (89%)	14/18 (78%)	NS
Thorax	62	59/62 (95%)	52/62 (84%)	44/62 (72%)	0.07
Abdomen	24	23/24 (96%)	20/24 (83%)	16/24 (67%)	NS
Pelvis	14	14/14 (100%)	13/14 (93%)	10/14 (71%)	NS
All	118	113/118 (96%)	101/118 (86%)	84/118 (71%)	<0.05

AC, Attenuation correction; NS, not significant

Table 2. Detection rate and lesion size

Diameter	Ring-PET		DH-PET		p-value
	AC (n)	no-AC	AC	no-AC	
≦20 mm	83	79/83 (95%)	66/83 (80%)	50/83 (60%)	<0.01
>20 mm	35	34/35 (97%)	35/35 (100%)	34/35 (97%)	NS

AC, Attenuation correction; NS, not significant

Table 3. Lesion characteristics

	DH-PET, attenuation-corrected			DH-PET, non-attenuation-corrected		
	Detected	Not detected	*P* value	Detected	Not detected	*P* value
SUV	10.7±5.8	9.4±7.3	NS	11.3±5.9	8.4±5.8	<0.01
Size[a] (mm)	22±13	14±4	<0.05	23±14	15±5	<0.001
l/bkg	2.7±2.2	1.8±0.9	<0.05	2.8±1.9	1.6±0.5	<0.001

l/bkg, lesion-to-background ratio

[a] estimated using "measure distance tool; ECAT 6.4"

strated 113 lesions (96%) in 35 patients. Attenuation-corrected DH-PET depicted 101 lesions (86%) in 34 patients, whereas only 84 lesions (71%) in 34 patients were shown by DH-PET without attenuation correction ($P<0.05$). DH-PET with and without attenuation correction was negative in all eight patients with negative attenuation-corrected ring PET.

Subdividing the lesions with respect to the anatomical localisation reveals an increase in the detection rate with attenuation-corrected (as compared with non-attenuation-corrected) DH-PET for all anatomical sites. Table 1 shows detection rates for different anatomical regions in detail. Subdividing the lesions with respect to lesion size shows an increase in detection rate for attenuation-corrected DH-PET for lesions ≤20 mm ($P<0.01$; Table 2).

The lesion-to-background ratios were significantly higher for ring PET than for DH-PET, both with (5.0±2.8 vs 2.6±2.0; $P<0.001$) and without attenuation correction (6.1±4.9 vs 2.5±1.7; $P<0.001$).

Lesions not detected by DH-PET showed a smaller diameter than did detectable lesions, for both attenuation-corrected and non-attenuation-corrected DH-PET. Lesions not detected with non-attenuation-corrected DH-PET showed lower SUVs than detectable lesions. Detailed data on these lesion characteristics are shown in Table 3. Attenuation correction slightly but significantly increased lesion-to-background ratios only for intrathoracic lesions (3.0±2.7 vs. 2.6±2.1; $P<0.01$).

Relative to attenuation-corrected ring PET as the standard of reference, concordant clinical findings were obtained with non-attenuation-corrected ring PET in 42 patients (93%), with attenuation-corrected DH-PET in 36 (80%) patients, and with non-attenuation-corrected DH-PET in 31 patients (69%). Combining attenuation-corrected and non-attenuation-corrected DH-PET resulted in findings concordant with attenuation-corrected ring PET in 37 patients (82%). Non-attenuation-corrected ring PET missed a focus suspicious for recurrent head and neck cancer, a lesion indicating an adrenal metastasis in lung

Table 4. Detection rates of lesions indicating (1) primary tumour/local recurrence, (2) lymph node metastases, (3) distant metastases or (4) involved lymph nodes in patients with malignant lymphoma. (Classification based on clinical data and localisation of the lesions; ten unclassified lesions not included)

	Ring-PET		DH-PET		*P* value*
	AC (*n*)	No AC	AC	No AC	
1) Primary tumour/ local recurrence	19	18/19 (95%)	18/19 (95%)	16/19 (84%)	NS
2) Lymph node metastases	30	29/30 (97%)	26/30 (87%)	20/30 (67%)	NS
3) Metastases	12	11/12 (92%)	8/12 (67%)	8/12 (67%)	NS
4) Involved lymph nodes (malignant lymphoma)	47	46/47 (89%)	43/47 (92%)	34/47 (72%)	<0.05

NS, Not significant

* Comparison of DH-PET with AC and DH-PET without AC

cancer and axillary lymph node involvement in a patient with low-grade malignant lymphoma. Attenuation-corrected DH-PET underestimated involved lymph nodes in four patients, metastatic spread in three patients and peritoneal carcinomatosis in one patient, and missed a lesion indicating local recurrence of renal cancer in one patient. Non-attenuation-corrected DH-PET underestimated involved lymph nodes in eight patients, metastatic spread in three patients, peritoneal carcinomatosis in one patient and local recurrence of renal cancer in one patient, and missed a lesion suspicious for recurrent head and neck cancer in one patient. These differences might have affected patient management in two patients (4%) for non-attenuation-corrected ring PET, six patients (13%) for attenuation-corrected DH-PET and ten patients (22%) for non-attenuation-corrected DH-PET (Table 4).

Discussion

In this study we evaluated a dual-head coincidence gamma camera equipped with ^{137}Cs sources for singles transmission attenuation correction in oncological FDG PET studies with attenuation-corrected ring PET as the standard of reference.

The lesion detection rate for non-attenuation-corrected DH-PET in this study (71%) is within the range of previously published results for dual-head coincidence gamma cameras of 55%–79% [12, 14, 15]. Besides lesion-to-background ratio and amount of FDG uptake, lesion size is one important factor determining detectability. In our study the detection rate for lesions ≤20 mm using non-attenuation-corrected DH-PET was only 60%, compared with 97% for lesions >20 mm. In contrast to this, the localisation of the lesions did not significantly influence detectability.

Measured attenuation correction using singles transmission markedly improves image quality, with better delineation of anatomical structures and absence of artefacts present on non-attenuation-corrected images (see Figs. 1–3). Attenuation correction significantly increased the lesion detection rate of DH-PET from 71% to 86% relative to attenuation-corrected ring PET. The improvement was especially evident for small lesions with a diameter ≤20 mm, with an increase of lesion detection rate from 60% to 80%. Measured attenuation correction improves lesion detectability in all body regions, e.g. head and neck area, thorax, abdomen and pelvis. This is mostly due to the clear improvement in image quality since the image contrast as expressed by the lesion-to-background ratios itself is positively affected by attenuation correction only for intrathoracic lesions surrounded by lung tissue (i.e. not for lesions outside the thorax).

The improvement in lesion detection capability is clinically relevant as the results concordant with attenuation-corrected ring PET increased from 78% for non-attenuation-corrected DH-PET to 87% for attenuation-corrected DH-PET.

The necessity of measured attenuation correction for ring PET is the subject of controversy. In this study, attenuation correction for ring PET had only a minor effect on both lesion detection and concordance of clinical results. This is in agreement with the observation by Kotzerke et al. that attenuation correction did not significantly improve the diagnostic accuracy of ring PET [23]. Bengel et al. reported a significantly higher lesion-to-background ratio for non-attenuation-corrected ring PET compared with attenuation-corrected ring PET [24]. More pragmatic arguments against conventional transmission studies are the considerable additional acquisition time required to achieve sufficient statistics and the problem of exact repositioning of the patient. However, without attenuation correction the shape of foci is distorted and exact anatomical localisation of the focus can be difficult, especially in the thorax [25]. Furthermore, increased FDG uptake of the lungs, the skin and those parts of the liver near to the surface are well-known artefacts of non-attenuation-corrected ring PET images. Moreover, attenuation correction is a precondition for quantitative image analysis (e.g. standardised uptake values).

Conclusion

Use of measured attenuation correction markedly improves image quality and minimises the limitations of

DH-PET for the detection of small lesions. This is achieved with only a minor increase in additional acquisition time. With singles transmission the diagnostic performance of DH-PET is closer to that of dedicated PET.

For dedicated ring PET the necessity of measured attenuation correction is still a matter of debate. However, since the introduction of segmented attenuation correction and singles transmission, the additional acquisition time required for attenuation correction is minimal. Because of the better image quality and the opportunity for quantification, measured attenuation correction is recommended for dedicated ring PET, too.

References

1. Rigo P, Paulus P, Kaschten BJ, Hustinx R, Bury T, Jerusalem G, Benoit T, Foidart-Willems J. Oncological applications of positron emission tomography with fluorine-18 fluorodeoxyglucose. *Eur J Nucl Med* 1996; 23: 1641–1674.
2. Conti PS, Keppler JS, Halls JM. Positron emission tomography: a financial and operational analysis. *Am J Roentgenol* 1994; 162: 1279–1286.
3. Drane WE, Abbott FD, Nicole MW, Mastin ST, Kuperus JH. Technology for FDG SPECT with a relatively inexpensive gamma camera. Work in progress. *Radiology* 1994; 191: 461–465.
4. Holle LH, Trampert L, Lung-Kurt S, Villena-Heinsen CE, Puschel W, Schmidt S, Oberhausen E. Investigations of breast tumors with fluorine-18-fluorodeoxyglucose and SPECT. *J Nucl Med* 1996; 37: 615–622.
5. Macfarlane DJ, Cotton L, Ackermann RJ, Minn H, Ficaro EP, Shreve PD, Wahl RL. Triple-head SPECT with 2-[fluorine-18]fluoro-2-deoxy-D-glucose (FDG): initial evaluation in oncology and comparison with FDG PET. *Radiology* 1995; 194: 425–429.
6. Martin WH, Delbeke D, Patton JA, Hendrix B, Weinfeld Z, Ohana I, Kessler RM, Sandler MP. FDG-SPECT: correlation with FDG-PET. *J Nucl Med* 1995; 36: 988–995.
7. Martin WH, Delbeke D, Patton JA, Sandler MP. Detection of malignancies with SPECT versus PET, with 2-[fluorine-18]fluoro-2-deoxy-D-glucose. *Radiology* 1996; 198: 225–231.
8. Mukherji SK, Drane WE, Mancuso AA, Parsons JT, Mendenhall WM, Stringer S. Occult primary tumors of the head and neck: detection with 2-[F-18] fluoro-2-deoxy-D-glucose SPECT. *Radiology* 1996; 199: 761–766.
9. Worsley DF, Celler A, Adam MJ, Kwong JS, Muller NL, Coupland DB, Champion P, Finley RJ, Evans KG, Lyster DM. Pulmonary nodules: differential diagnosis using ^{18}F-fluorodeoxyglucose single-photon emission computed tomography. *Am J Roentgenol* 1997; 168: 771–774.
10. Trampert L, Holle LH, Berberich R, Alexander C, Ukena D, Ruth T, Sybrecht GW, Oberhausen E. ^{18}FDG in the primary staging of lung tumors. Results with a gamma camera and a 511 keV collimator. *Nuklearmedizin* 1995; 34: 79–86.
11. Lonneux M, Delval D, Bausart R, Moens R, Willockx R, Mael PV, Declerck P, Jamar F, Zreik H, Pauwels S. Can dual-headed 18F-FDG SPET imaging reliably supersede PET in clinical oncology? A comparative study in lung and gastrointestinal tract cancer. *Nucl Med Commun* 1998; 19: 1047–1054.
12. Shreve PD, Steventon RS, Deters EC, Kison PV, Gross MD, Wahl RL. Oncologic diagnosis with 2-[fluorine-18]fluoro-2-deoxy-D-glucose imaging: dual-head coincidence gamma camera versus positron emission tomographic scanner. *Radiology* 1998; 207: 431–437.
13. Schwaiger M, Ziegler S. PET using a coincidence camera versus ring tomography, progress or recession? [editorial]. *Nuklearmedizin* 1997; 36: 3–5.
14. Delbeke D, Patton JA, Martin WH, Sandler MP. FDG PET and dual-head gamma camera positron coincidence detection imaging of suspected malignancies and brain disorders. *J Nucl Med* 1999; 40: 110–117.
15. Zimny M, Kaiser HJ, Cremerius U, Sabri O, Schreckenberger M, Reinartz P, Buell U. Fluorine-18-fluorodeoxyglucose positron imaging in oncological patients: gamma camera coincidence detection versus dedicated PET. *Nuklearmedizin* 1999; 38: 108–114.
16. Stokkel MP, Terhaard CH, Mertens IJ, Hordijk GJ, van Rijk PP. Fluorine-18-FDG detection of laryngeal cancer postradiotherapy using dual-head coincidence imaging. *J Nucl Med* 1998; 39: 1385–1387.
17. Karp JS, Muehllehner G, Qu H, Yan XH. Singles transmission in volume-imaging PET with a ^{137}Cs source. *Phys Med Biol* 1995; 40: 929–944.
18. Yu SK, Nahmias C. Single-photon transmission measurements in positron tomography using ^{137}Cs. *Phys Med Biol* 1995; 40: 1255–1266.
19. Shao L, Nellemann P, Muehllehner G, Bertelsen H, Hines H. Singles-transmission attenuation correction for dual head coincidence imaging. *J Nucl Med* (*Suppl*) 1998; 39: 37P.
20. Shepp LA, Vardi Y. Maximum likelihood reconstruction for positron emission tomography. *IEEE Trans Med Imaging* 1982; 2: 113–122.
21. Lewellen TK, Miyaoka RS, Swan WL. PET imaging using dual-headed gamma cameras: an update. *Nucl Med Commun* 1999; 20: 5–12.
22. Thill R, Neuerburg J, Fabry U, Cremerius U, Wagenknecht G, Hellwig D, Osieka R, Gunther R, Bull U. Comparison of findings with 18-FDG PET and CT in pretherapeutic staging of malignant lymphoma (in German). *Nuklearmedizin* 1997; 36: 234–239.
23. Kotzerke J, Guhlmann A, Moog F, Frickhofen N, Reske SN. Role of attenuation correction for fluorine-18 fluorodeoxyglucose positron emission tomography in the primary staging of malignant lymphoma. *Eur J Nucl Med* 1999; 26: 31–38.
24. Bengel FM, Ziegler SI, Avril N, Weber W, Laubenbacher C, Schwaiger M. Whole-body positron emission tomography in clinical oncology: comparison between attenuation-corrected and uncorrected images. *Eur J Nucl Med* 1997; 24: 1091–1098.
25. Zasadny KR, Kison PV, Quint LE, Wahl RL. Untreated lung cancer: quantification of systematic distortion of tumor size and shape on non-attenuation-corrected 2-[fluorine-18]fluoro-2-deoxy-D-glucose PET scans. *Radiology* 1996; 201: 873–876.